Ecological Modelling 521 (2026) 111716

Contents lists available at ScienceDirect

Ecological Modelling

journal homepage: www.elsevier.com/locate/ecolmodel

me4soc: a multi-model ensemble interface for soil organic carbon predictions

Elisa Bruni [a,*], Aleksi Lehtonen [b], Shoji Hashimoto [c,d], Boris Ťupek [b], Nasser Bacha [a], Daniel Bunker [e], Illian Brasselet-Darracq [a], Dalia Fages-Gouyou [a], Yanis Hemeray [a], Christopher P.O. Reyer [f], Carlos A. Sierra [g], Bertrand Guenet [a]

[a] *Laboratoire de Geologie ENS, PSL Research University, CNRS, UMR 8538, IPSL, Paris, France*
[b] *Bioeconomy and environment unit, Natural Resources Institute Finland (Luke), Helsinki, 00790, Finland*
[c] *Department of Forest Soils, Forestry and Forest Products Research Institute, Tsukuba, Ibaraki, 305-8687, Japan*
[d] *Graduate School of Agricultural and Life Sciences, The University of Tokyo, Bunkyo-ku, Tokyo, 113-8657, Japan*
[e] *Department of Biological Sciences, New Jersey Institute of Technology, Newark, NJ, USA*
[f] *Potsdam Institute for Climate Impact Research (PIK), Member of the Leibniz Association, Potsdam, Germany*
[g] *Max Planck Institute for Biogeochemistry, Jena, Germany*

A R T I C L E I N F O

Dataset link: https://github.com/elisabruni/me4soc

Keywords:
Soil organic carbon
me4soc
Climate change
Land-use change
Climate-smart management
Multi-model ensemble

A B S T R A C T

Model predictions are essential to understand how climate and land management affect soil organic carbon (SOC) stocks and greenhouse gases (GHGs). However, large uncertainties remain, and multi-model ensembles are a key approach to account for the uncertainty associated with model structure.

We present *me4soc* (Multi-model Ensemble interface for Soil Organic Carbon predictions), an open-source web application designed to simulate SOC stocks and GHG fluxes at mineral-soil forest sites under varying climate, land-use, and management scenarios. The platform runs six SOC models, using either user-supplied observations or preprocessed open-access European datasets. Simulations incorporate projections from Earth System Models to account for future climate and land-use trajectories. Developed in Shiny (R), *me4soc* simulates the temporal dynamics of site-level SOC stocks and GHG emissions and allows to quantify the uncertainty linked to model structure. It is intended for researchers and forest managers to support decision-making by examining how climate-smart management can affect forest soils through changes in plant litter inputs.

1. Introduction

Soil is the largest carbon (C) pool among terrestrial ecosystems and stores more C than vegetation and atmosphere combined (Lal, 2008; Jackson et al., 2017; Friedlingstein et al., 2025). However, the global distribution of soil organic carbon (SOC) stocks is strongly influenced by land-use, with forests accounting for approximately 75% of global SOC stocks in the top 2 meters of soil – including forests in permafrost and peatland regions (Jackson et al., 2017) – making forests a key component of the global C cycle.

Forest health is increasingly threatened by human activities and climate change, with associated risks of SOC losses and increased greenhouse gas (GHG) emissions. The conversion of forests to other land-uses is one of the principal causes of human-induced SOC depletion (Lal, 2004). Climate-driven disturbances such as droughts, insect outbreaks, and wildfires, as well as intensive human interventions for harvesting, like clear-cutting and the removal of harvest residues, can also significantly reduce SOC stocks (Mäkipää et al., 2023). In contrast, climate-smart forest management practices have the potential to enhance forest SOC storage, reduce GHG emissions, increase forest resilience, and secure wood production (Pan et al., 2024). Hence, a comprehensive understanding of the effect of climate, land-use and forest management is essential for developing sustainable mitigation approaches.

SOC models (e.g., Manzoni et al., 2012; Le Noë et al., 2023) are needed to predict the effect of land-use and forest management on SOC stocks and GHG emissions under current and future climate. However, model predictions are still highly uncertain. For example, Todd-Brown et al. (2013) reported large variations in SOC simulations among Earth System Models from the fifth Coupled Model Intercomparison

* Corresponding author.
E-mail address: bruni@geologie.ens.fr (E. Bruni).

https://doi.org/10.1016/j.ecolmodel.2026.111716
Received 8 November 2025; Received in revised form 3 May 2026; Accepted 20 June 2026
Available online 1 July 2026

Project (CMIP5), and virtually no improvements were observed in the last CMIP6 simulations (Varney et al., 2022). One way to assess uncertainty in model predictions is to use multi-model ensembles to account for different model structures and mechanistic assumptions (Sierra et al., 2012; Riggers et al., 2019; Farina et al., 2021; Bruni et al., 2022). This approach is used, for instance, in the climate projections of the Intergovernmental Panel on Climate Change (IPCC) (Pachauri et al., 2015). Assessing uncertainty in SOC model predictions is particularly important since they are used to inform policy makers and forest managers on the best land management practices for climate change mitigation. However, the use of SOC models – and especially multi-model ensembles – requires a number of technical resources and data that are not always available to these stakeholders. Hence, efforts to develop robust yet user-friendly tools for decision support is a critical step to improve forest management and predictions. This need is further amplified by the rise of voluntary carbon markets for climate change mitigation, where reliable and user-friendly tools are crucial for monitoring SOC changes and supporting credible C removals (Smith et al., 2020). Despite their importance, tools that can make ensemble modeling accessible to non-experts—such as forest managers and policy makers—are lacking.

Here, we present *me4soc*, a *Multi-model Ensemble interface for Soil Organic Carbon predictions* (Fig. 1). *Me4soc* is an easy-to-use open-source web application that allows users to run an ensemble of six SOC models under different climate, land-use and land management change scenarios (Fig. 2). SOC models include both process-based models (Century, Parton et al., 1988; Roth-C, Coleman and Jenkinson, 1996; ICBM, Andrén and Kätterer, 1997; Yasso07, Tuomi et al., 2009; and Yasso20, Viskari et al., 2022) and empirical models (SG, Hashimoto et al., 2011). Forcing data can be input by the user or, when not available, for the European region data is directly extracted from large scale open-source datasets. This allows end users to predict the evolution of SOC stocks and GHG emissions even when all the data is not available. *Me4soc* enables stakeholders to explore the impacts of management decisions on SOC trends under different climate change scenarios. In particular, this tool supports forest managers and policy makers in optimizing forest management practices - such as thinning intensity, rotation length, and use of harvest residues - to reduce SOC losses in forest soils. It can support applications including forest planning, carbon credit reporting, GHG emission inventorying, and the design of effective mitigation strategies – provided prior validation against local conditions is performed (IPCC, 2019). To our knowledge, *me4soc* is the first tool to provide site-specific, scenario-based SOC ensemble projections via an intuitive and open-source web interface. With *me4soc*, we aim to bridge the gap between advanced SOC modeling and decision-making needs, promoting evidence-based forest management in a changing climate.

2. Environment description

2.1. Software environment

The web application *me4soc* was developed using the Shiny framework (R Core Team, 2022) and is publicly available via a server hosted at the École Normale Supérieure de Paris (http://me4soc.geologie.ens.fr/). It includes a demo version that runs fast but contains data for a limited number of sites, and a full version (*me4soc* v1), which includes data for the entire European region and therefore requires large memory resources.

2.2. Interface

The interface has a clear and user-friendly structure with a sidebar menu including different sections: "Description", "Data", "Outputs", and "About" (Fig. 1). In particular, the "Description" panel presents the project objectives, the datasets processed for data extraction, the models used for the simulations, and the climate, land-use and land management change scenarios implemented. The "Data" panel allows the user to input the data for model simulations or, by selecting the geographical coordinates of the site of interest, extract the data from open-source databases that were pre-processed and pre-stored in the server. The "Outputs" panel generates plots for the visualization of the data input, and allows the user to run the models to simulate SOC stocks and GHG emissions at the selected site. Finally, the "About" panel includes a

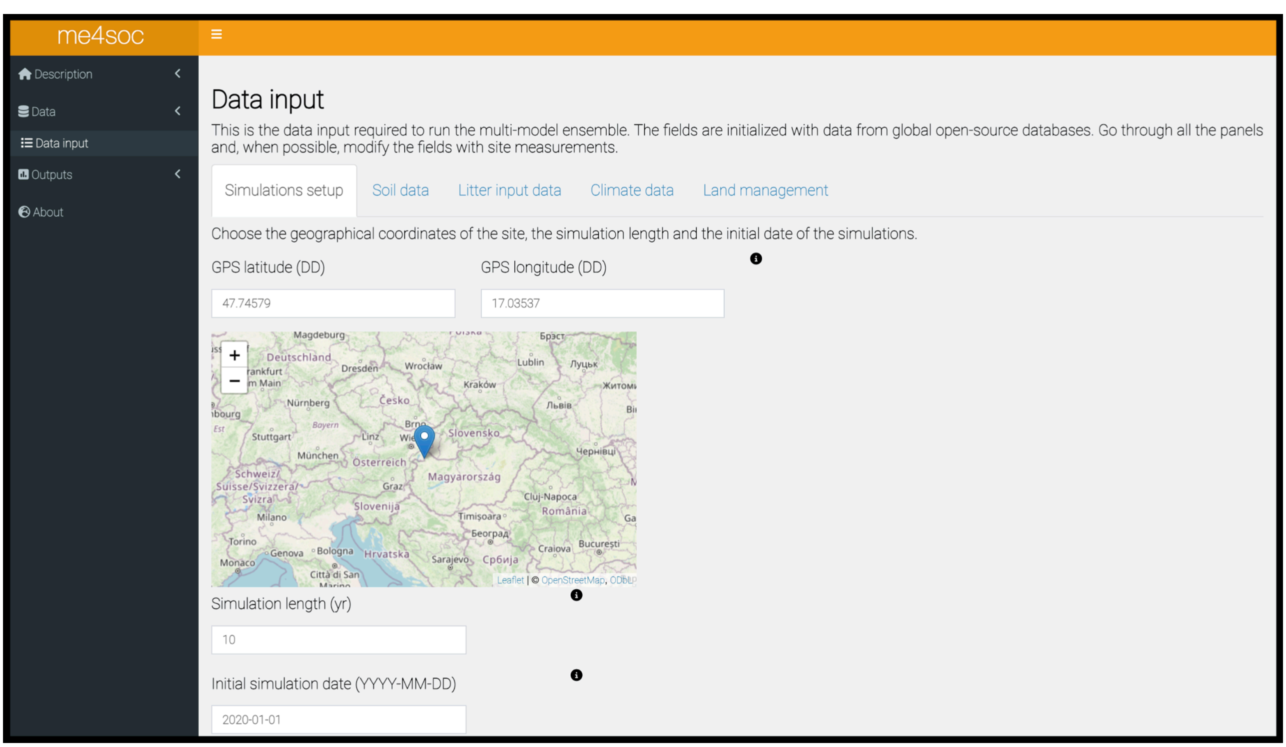

Fig. 1. Screenshot of the webapp interface. On the left, the sidebar menu and on the right the data input landing page.

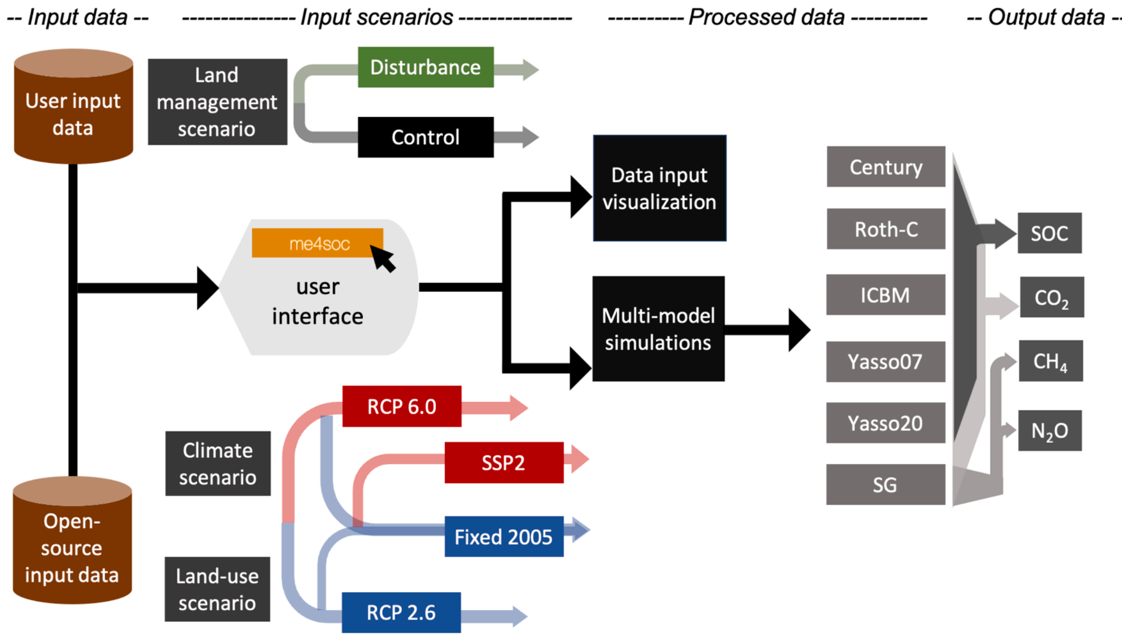

Fig. 2. Schematization of the *me4soc* web application environment, including input data, input scenarios, processed data, and output data. Data input sources are either user-based or extracted from open-source databases. Input scenarios include land management (disturbance denoting natural disturbances and forest management, and control being the business-as-usual scenario), climate scenarios are based on RCP 2.6 and RCP 6.0, and land-use is either fixed to year 2005, or varying according to SSP2. Data is processed for visualization and to launch the multi-model ensemble that includes Century, Roth-C, ICBM, Yasso07, Yasso20, and SG, which simulate SOC (all models except SG), CO_2 (all models), CH_4 (SG) and N_2O (SG).

tutorial, the documentation of the web application, the GitHub link to the web application code, the license, and various bibliographic references.

3. Models

The multi-model ensemble includes five SOC models (Fig. 3) and one empirical model allowing for the estimation of GHG fluxes (CO_2, N_2O, and CH_4).

3.1. Simulation of SOC stocks

The SOC models represent SOC with a conventional multi-compartmental structure that can be summarized with the following matrix equation:

$$\frac{d\boldsymbol{C}(t)}{dt} = \boldsymbol{I}(t) - \xi(t)\cdot\mathbf{A}\cdot\mathbf{K}\cdot\boldsymbol{C}(t),\ \ \boldsymbol{C}(t=0) = \boldsymbol{C}_0, \tag{1}$$

Where $\boldsymbol{C}(t)$ is a nx1 element vector describing the soil organic carbon

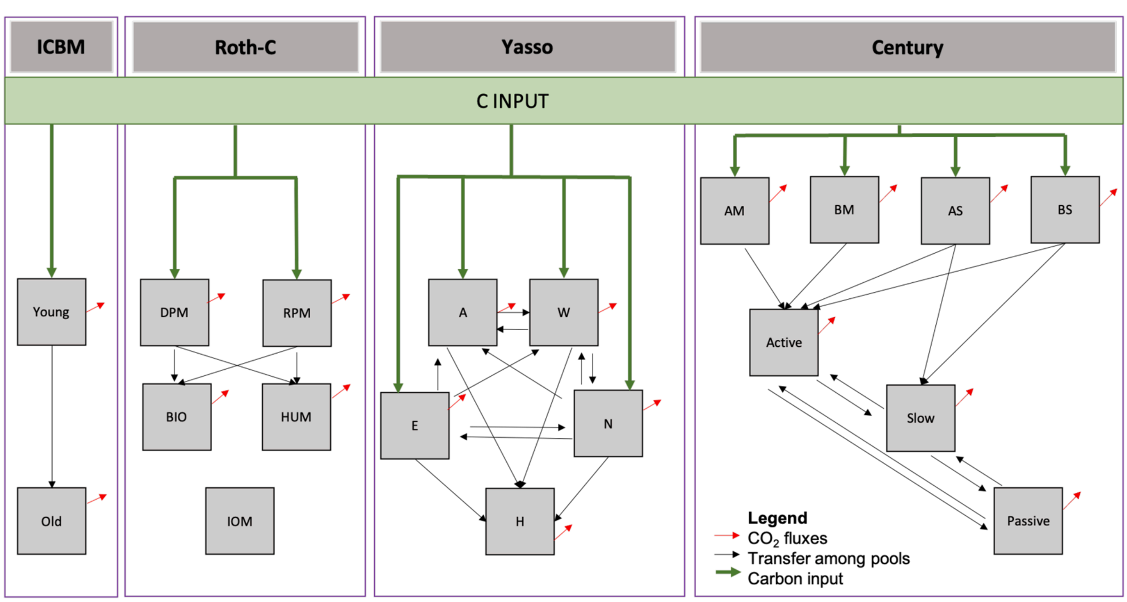

Fig. 3. Schematization of the SOC models used in the ensemble. Each box represents a SOC compartment where the C is transferred (black arrows), or respired to the atmosphere (red arrows). DPM, RPM, BIO, HUM, and IOM represent the decomposable plant material, resistant plant material, microbial biomass, humified organic matter, and inert organic matter pools of the Roth-C model, respectively. A, W, E, N, and H represent the acid hydrolysable, water soluble, ethanol soluble, neither soluble nor hydrolysable, and humus compound fractions of the Yasso07 and Yasso20 models, respectively. AM, BM, AS, BS represent the aboveground metabolic, belowground metabolic, aboveground structural, and belowground structural pools of the Century model, respectively.

stock in the n model compartments as a function of time (t) and $dC(t)/dt$ its derivative over time; $I(t)$ is a nx1 element vector representing the amount of C input to the soil compartments; $\xi(t)$ is a scalar-valued function representing the effect of the pedo-climatic conditions on the decomposition of SOC; **A** is a nxn matrix describing the mass flow between compartments, with each element $a_{i,j}$ representing the flow of SOC from compartment j to compartment i (with $i,j = 1,\dots, n$); **K** is a nxn diagonal matrix containing the decomposition rate coefficients of the n compartments; and C_0 is a nx1 vector representing the level of SOC in each compartment at the beginning of the simulations (i.e., when $t = 0$).

3.2. Simulation of CO_2 fluxes

The CO_2 fluxes can be calculated from the SOC models as,

$$r = \mathbf{R}\cdot C(\mathrm{t}), \tag{2}$$

with r being the instantaneous release of C for all n compartments, and **R** being a nxn diagonal matrix having the release coefficients r_j calculated from matrix **A** as: $r_j = 1 - \sum_{i=1}^{n} (a_{i,j})$.

3.3. Models in the ensemble

We used five SOC models, all based on the linear non-autonomous formulation of SOC pool decomposition described in Eq. (1), but differing in structural complexity. In particular, these models differed by the number of compartments (n), the transfer rates between compartments (**A**), the environmental scalar functions ($\xi(t)$), and the decomposition rate coefficients (**K**). The models included were: ICBM (Andrén and Kätterer, 1997), Roth-C (Coleman and Jenkinson, 1996), Yasso07 (Tuomi et al., 2009), Yasso20 (Viskari et al., 2022), and Century (Parton et al., 1988). Yasso07 and Yasso20 share the same model structure; however, a key distinction is that Yasso20 incorporates pool-specific environmental scalar functions. Model structures are schematized in Fig. 3 and specific information on each model can be found in their reference paper and in the SoilR package documentation (Sierra et al., 2012). These models were chosen to balance (i) conceptual diversity in SOC representations, ranging from simple two-pool model formulations to more process-based and litter-quality-driven approaches, (ii) demonstrated applicability to predict forest SOC stocks across multiple regions (Garsia et al., 2023), and (iii) compatibility with user-driven simulations in terms of both computational efficiency and input data requirements.

3.4. Model resolution

The models were solved numerically using the 'lsoda' integrator from the R package 'deSolve', a solver for ordinary differential equations (ODEs) already implemented in SoilR (Sierra et al., 2012). 'lsoda' uses an adaptive time-stepping scheme, where internal steps are automatically adjusted to satisfy absolute and relative error tolerances (set to 10^{-6}), to ensure numerical accuracy. Each model has an intrinsic temporal resolution determined by the units of its processes (e.g., annual decomposition rates). However, to ensure the output captured these dynamics with high precision, the solution was recorded at a finer frequency (1/365 year). The ODEs were solved for the specified simulation length with input data provided by the user.

Solving the ODEs requires specifying the initial conditions of the system (C_0). Since the partitioning of C among the conceptual soil compartments cannot be directly measured, we estimated the initial pool sizes by simulating pre-experimental conditions. Models were run for 5000 years under constant C inputs (I) and climate forcing (ξ), until all compartments reached steady-state. Operationally, steady-state was defined as when the relative change in each SOC pool between time steps was lower than 0.1% for at least 10 consecutive years. Climate forcing was set to the 15-year mean preceding the start of the experiment. We rescaled the simulated steady-state SOC to match the total measured SOC at the beginning of the experiment, preserving the relative proportions of C among pools (Hashimoto et al., 2011; Dimassi et al., 2018). The rescaled stocks were used as initial conditions for the simulations.

3.5. Simulation of other GHG fluxes

In addition to the CO_2 fluxes, CH_4 uptake and N_2O fluxes are also estimated using the SG models (Hashimoto et al., 2011). These are simple empirical models that estimate GHG fluxes using data on soil physiochemical properties (SP), water-filled pore space (WFPS), and soil temperature (T) in the 0-5 cm soil layer:

$$GHG = f(SP)\; g(WFPS)\; h(T) \tag{3}$$

Where GHG is either CO_2, CH_4, or N_2O flux; $f(SP)$ is the function of physiochemical properties, $g(WFPS)$ is the function of water-filled pore space, and $h(T)$ is the function of soil temperature.

The $f(SP)$ function has the same exponential shape for all gases ($f(SP) = m_1\, e^{m_2\, SP}$), but the SP variable changes according to the gas (i. e., SP is the C:N ratio for CO_2 and N_2O, while SP is the bulk density for CH_4) The m_1 and m_2 absolute values are the same for all gases, but m_2 has a negative sign for both CH_4 and N_2O, indicating a decrease in the gas flux with increasing bulk density and C:N, respectively. For all gas fluxes, $g(WFPS)$ has a convex shape and is computed as: $g(WFPS) = [(WFPS - a)\ /(b - a)]^d [(WFPS - c)\ /(b - c)]^{-d((b-c)/(b-a))}$, with a, b, c, and d the parameters. In the absence of measured $WFPS$, volumetric water content (θ) and bulk density (BD) can be used to estimate it, as: $WFPS = \theta/(1 - (BD/2.65)$. Finally, $h(T)$ also has an exponential form and is the same for all gases ($h(T) = e^{pT}$, with p the parameter). All parameters were empirically determined with Bayesian calibration on 36 Japanese forested sites under various pedo-climatic conditions (Hashimoto et al., 2011), and these are used as default values in *me4soc*. The model has already been successfully implemented at the global scale (Hashimoto, 2012) and is currently integrated into the biogeochemical model Biome-BGC MUSO (Hidy et al., 2016). While the original calibration was performed on Japanese forest ecosystems, its application to European sites assumes a degree of process generality across temperate systems; this may introduce regional biases, which are acknowledged as a limitation of the present study.

4. Data

The data required to run the models can either be uploaded by the user or, if not available, automatically provided by the webapp using pre-processed data from open-source datasets (Table 1). This automatic option is currently available only for Europe. The following sections describe the data input requirements, the data sources used for the automatic option in Europe, and the procedures applied to derive the variables from the open-source databases.

Table 1
References and sources of the online open-source repositories used to extract the required data to launch the models.

Short-name	Reference	Variables	Resolution
ISIMIP	(Frieler et al., 2017; Reyer et al., 2019)	Climate, Net primary production, Biomass	0.5°
TRY	(Kattge et al., 2020)	Litter quality	Global
LUCAS	(De Brogniez et al., 2015; Ballabio et al., 2016, 2019; Yigini and Panagos, 2016)	Soil	500 m (1000 m for SOC stock)
GML	(Lan et al., 2022)	Atmospheric CH_4	Global

4.1. Data input requirements

The different models require a wide range of input data (Table A1) to simulate the evolution of SOC stocks and GHG fluxes over time. These data include information on the simulation set-up (e.g., initial date and length of the simulation), site-specific pedo-climatic conditions, litter inputs, and land management practices. In particular, soil data include texture, soil C and nitrogen (N) content, bulk density, and layer depth. Litter input data cover the dominant tree species, amounts of aboveground and belowground C inputs over the simulation period, the chemical quality of the litter input, and the size of woody debris. Climate data consist of daily air temperature, precipitation, volumetric soil water content, and monthly potential evapotranspiration during the simulation period. In addition, average climate conditions over the decades preceding the simulations are needed to initialize the models. Atmospheric data include the concentration of CH_4 at the start of the simulations, which is required to run the SG models. Land management data comprise the year of the disturbance event (e.g., thinning, clear-cutting, or disease outbreaks), as well as aboveground and belowground tree biomass before the disturbance, tree mortality rate and harvest rate of the dead aboveground biomass. The web application provides definitions for all variables, and instructions for their preparation. Additional information for the user is available in the documentation that can be downloaded from the website. Data input requirements are also listed in Table A1.

4.2. Open-source data

When the geographic coordinates of the site are selected, the tool automatically extracts soil, litter and climate data from pre-processed regional and global databases (Table 1). That is, the Inter-Sectoral Impact Model Intercomparison Project (ISIMIP) database, protocol 2b (Frieler et al., 2017) for climate and litter C input data, the European LUCAS database (De Brogniez et al., 2015; Ballabio et al., 2016, 2019; Yigini and Panagos, 2016) for soil measurements and derived products (0-20 cm depth), the Plant Trait (TRY) database (Kattge et al., 2020) and Yasso manual (Liski et al., 2009) for species-specific litter chemical properties, and the Global Monitoring Laboratory (GML) database for mean annual global marine atmospheric CH_4 concentration (Lan et al., 2022). This feature allows the models to be run over European sites even if all the required data is not available. However, measured site data should always be prioritized, when possible. Table A1 details the data sources of each variable for this automatic option, indicating whether values were directly extracted or estimated.

5. Scenarios

We implemented different climate, land-use and land management change scenarios in order to simulate their effect on the SOC stocks and GHG emissions with the multi-model ensemble.

5.1. Climate change scenarios

Climate change scenarios were built from the representative concentration pathways (RCPs) described in the Fifth Assessment Report (AR5) of the Intergovernmental Panel on Climate Change (IPCC) (Pachauri et al., 2015). In particular, we focused on RCP 2.6 and RCP 6.0, which predict an average global land temperature increase of 1 °C and 2.2 °C during the period 2081-2100, compared to mean temperatures in 1986-2005, respectively. To achieve this, we forced the SOC models with climate and litter C input data (Table 2) derived from ISIMIP model simulations under the two RCP scenarios (Frieler et al., 2017) for the period 2020-2099. For model spin-up, average climate data between 2006 and 2020 was used. Daily precipitation and temperature were derived from simulations of two climate models (i.e., ipsl-cm5a-lr and miroc5, Table 2), which were then averaged to obtain the multi-model mean daily precipitation and temperature. A simple mean was taken because ISIMIP climate inputs were already bias-adjusted using observed data. Monthly potential evapotranspiration and daily soil moisture were derived from simulations of the same two climate models, coupled with the land-surface model ORCHIDEE (Krinner et al., 2005), and similarly averaged to obtain the multi-model mean (Table 2). Hence, the climate forcing variables used in the web application are multi-model averages of global model simulations. The models from which the simulated data was extracted are listed in Table 2 for each forcing variable. After extraction, daily data was converted to a monthly timescale to reduce the data size of the web application.

Table 2
Models of the ISIMIP repository used to estimate the multi-model average climate and vegetation forcing. The units and time frequency refer to the values extracted from the ISIMIP repository.

Variable	Unit	Climate model	Vegetation model
Daily mean precipitation	kg m^{-2} s^{-1}	ipsl-cm5a-lr, miroc5	
Daily mean air temperature	°K	ipsl-cm5a-lr, miroc5	
Monthly mean potential evapotranspiration	kg m^{-2} s^{-1}	ipsl-cm5a-lr, miroc5	orchidee
Monthly mean soil moisture (top 18 cm)	kg m^{-2}	ipsl-cm5a-lr, miroc5	orchidee
Annual mean net primary production	kg C m^{-2} s^{-1}	ipsl-cm5a-lr, miroc5	dlem, lpj-guess
Total aboveground vegetation biomass	kg C m^{-2}	ipsl-cm5a-lr, miroc5	dlem, lpj-guess

5.2. Land-use change scenarios

The land-use change scenarios are derived from the shared socio-economic pathways (SSPs) defined in the IPCC Sixth Assessment Report (AR6) (Masson-Delmotte et al., 2021). In particular, we focused on the SSP2, which contemplates social, economic and technological trends that do not shift markedly from historical patterns. To achieve this, we forced the models with vegetation biomass data produced by the ISIMIP vegetation models between 2006 and 2099, under 1) a fixed year-2005 land-use, nitrogen deposition and fertilizer input scenario (i.e., 2005soc in Frieler et al., 2017), and 2) a varying land-use, water abstraction, nitrogen deposition and fertilizer input scenario according to SSP2 (i.e., rcpsoc in Frieler et al., 2017). The annual net primary production (NPP) and the total aboveground tree biomass were derived from simulations of two climate models (i.e., ipsl-cm5a-lr and miroc5) coupled with two land-surface models (i.e., dlem and lpj-guess, Table 2), and averaged (Table 2). These land-surface models were selected because they included the necessary vegetation variables, defined independently of plant functional type to reduce storage requirements. The annual NPP variable was used to estimate the aboveground and belowground C input, while total aboveground vegetation biomass was used to estimate the increase in C input during a mortality event (see subsection 5.3). We selected the period 2006-2020 of RCP 2.6 with fixed year-2005 land-use for SOC model spin-up, and the period 2020-2099 for forward runs with the different climate and land-use change scenarios.

5.3. Land management change scenarios

The land management change scenario considers a user-defined natural or harvest disturbance event such as cutting, thinning, or tree disease, after which some of the vegetation dies and is partly removed from the soil. The assumptions made to estimate the C input to the soil during the disturbance event and for the rest of the years of the simulation are schematized in Fig. 4, and detailed below.

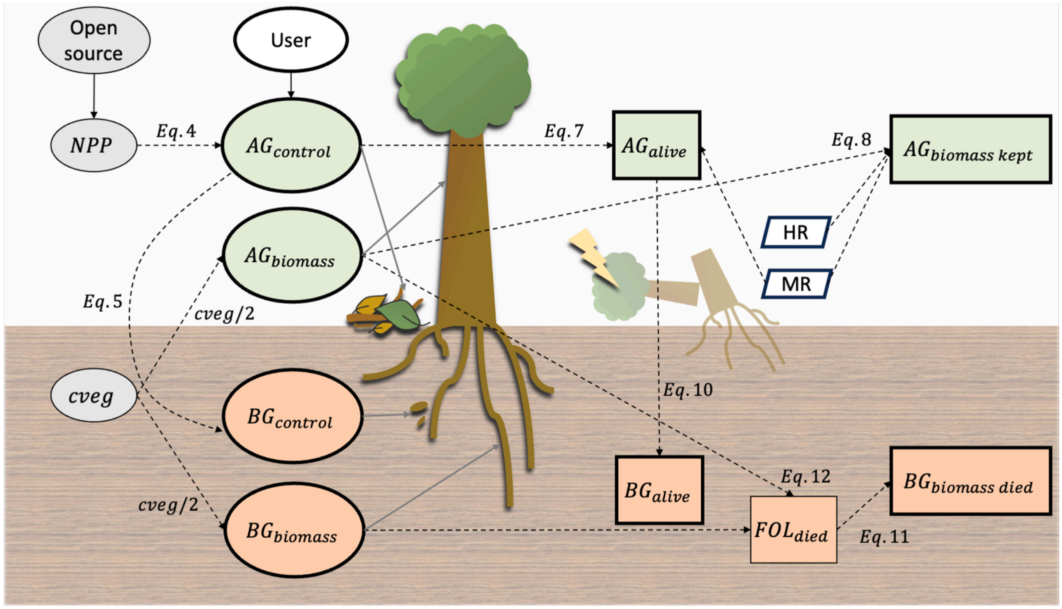

Fig. 4. Representation of the assumptions made to calculate the litter input following a disturbance event. Grey circular boxes represent input data extracted from open-source databases, while circular boxes with black borders indicate user-provided variables. Square boxes denote variables estimated within the web application; among these, those with black borders are used to calculate the total litter input under the disturbance treatment. Dashed arrows indicate relationships between variables, with corresponding equation numbers shown.

5.3.1. Control scenario

The annual aboveground and belowground C input to the soil is either input by the user or calculated from NPP, derived from ISIMIP simulations, protocol 2b (Frieler et al., 2017). Note that NPP from ISIMIP simulations represents total NPP under natural conditions and does not necessarily capture specific plant functional types. Following Malhi et al. (2011), aboveground litter C input $(\mathrm{MgC\ ha^{-1}yr^{-1}})$ is estimated from NPP (Neumann et al., 2018) as:

$$AG_{control} = \mathrm{NPP} \times 0.34, \tag{4}$$

where the NPP variable was converted from ISIMIP outputs to $\mathrm{MgC\ ha^{-1}yr^{-1}}$ (Table 2), for both RCP 2.6 and RCP 6.0 scenarios.

Belowground litter C input $(\mathrm{MgC\ ha^{-1}yr^{-1}})$ is then estimated from the aboveground litter C input with the equation from Jonard et al. (2017), as:

$$BG_{control} = 0.333 \times \left(1.92 \times AG_{control} \times \left(\mathrm{conversion_{factor}}\right) + 130\right) / \left(\mathrm{conversion_{factor}}\right), \tag{5}$$

where $\mathrm{conversion_{factor}}$ is the conversion factor from $\mathrm{MgC\ ha^{-1}}$ to $\mathrm{gC\ m^{-2}}$.

5.3.2. Disturbance scenario

We assume that the aboveground C input of the disturbance scenario $(\mathrm{MgC\ ha^{-1}yr^{-1}})$ is equal to:

$$AG_{disturbance} = \begin{cases} AG_{control}, & for\ t < D \\ AG_{alive}, & for\ t > D \\ AG_{alive} + AG_{biomass\ kept}, & for\ t = D \end{cases}, \tag{6}$$

where: D is the year of the disturbance (natural or management) and t is time; AG_{alive} is the aboveground C input from alive vegetation, computed as,

$$AG_{alive} = AG_{control} \times \left(1 - \frac{\mathrm{MR}}{100}\right) \tag{7}$$

where MR is the user-input mortality rate (%), defined as the percentage of vegetation died due to the disturbance; and $AG_{biomass\ kept}$ is the dead aboveground biomass that is kept in the soil, computed as,

$$AG_{biomass\ kept} = AG_{biomass} \times \frac{\mathrm{MR}}{100} \times \left(1 - \frac{\mathrm{HR}}{100}\right), \tag{8}$$

with $AG_{biomass}$ being the aboveground vegetation biomass of the year preceding the disturbance event and HR the user-input harvest rate (%), defined as the percentage of vegetation removed from the soil after the disturbance. $AG_{biomass}$ is either input by the user or calculated as: $cveg/2$, where $cveg$ is the total vegetation biomass under natural conditions of the year previous to the disturbance event, extracted from multi-model average simulations from the ISIMIP repository (Table 2). Note that we do not explicitly distinguish between natural or management disturbance. However, the user can set the harvest rate (HR) to 0% to mimic a natural disturbance with no post-disturbance harvest.

The belowground C input of the disturbance scenario $(\mathrm{MgC\ ha^{-1}yr^{-1}})$ is then calculated as:

$$BG_{disturbance} = \begin{cases} BG_{control}, & for\ t < D \\ BG_{alive}, & for\ t > D \\ BG_{alive} + BG_{biomass\ died}, & for\ t = D \end{cases}, \tag{9}$$

where: BG_{alive} $(\mathrm{MgC\ ha^{-1}yr^{-1}})$ is the belowground C input from alive vegetation and is computed following Jonard et al. (2017) as,

$$BG_{alive} = 0.333 \times 1.92 \times AG_{alive} \times \left(\mathrm{conversion_{factor}}\right) + 130 / \left(\mathrm{conversion_{factor}}\right) \tag{10}$$

$BG_{biomass\ died}$ $(\mathrm{MgC\ ha^{-1}yr^{-1}})$ is the dead aboveground biomass kept in the soil, similarly computed as,

$$BG_{biomass\ died} = 0.333 \times \left(1.92 \times FOL_{died} \times \left(\mathrm{conversion_{factor}}\right) + 130\right) / \left(\mathrm{conversion_{factor}}\right), \tag{11}$$

with FOL_{died} $(\mathrm{MgC\ ha^{-1}yr^{-1}})$ being the dead foliar litter computed, following Konôpka et al. (2021), as,

$$FOL_{died} = 0.15 \times (AG_{biomass} + BG_{biomass}) \times \frac{MR}{100}, \tag{12}$$

and $AG_{biomass}$ and $BG_{biomass}$ being the aboveground and belowground vegetation biomass of the year preceding the disturbance event, respectively, which are either input by the user, or both estimated as: $cveg/2$. It is assumed that all the dead belowground biomass is kept in the soil, i.e., the harvest rate does not affect the belowground part of the vegetation.

6. Example simulation

We present a case study to illustrate the functionalities of the web application, using only data from the open-source databases. In particular, we simulate a 10-year period for a site located in the French Manson Forest (45° 45' 20" N, 2° 57' 58" E), dominated by *Picea Abies*. The site is part of the French forest monitoring network (RENECOFOR) and more information can be found in Jonard et al. (2017).

In the land management scenario, we simulate a thinning disturbance occurring in the first year (i.e., 2020), characterized by a 50% tree harvest. This corresponds to a 50% tree mortality rate (MR) and a 100% harvest rate (HR) applied to the dead aboveground biomass. This scenario represents for example a high intensity thinning event, with residue removal. As shown in Fig. 5, this scenario leads to a sharp increase in C inputs in the first year, followed by a decrease from the second year onward, compared to the control scenario. The initial increase in C input is driven by the mortality event, which contributes to a rise in dead belowground biomass directly transferred to the soil (Eq. 9). The subsequent decline is due to the full removal (100% harvest) of the dead aboveground biomass. With only 50% of the trees remaining after the disturbance, the total C input is therefore lower than the control.

6.1. *Intense thinning decreases the SOC stocks*

The multi-model mean simulations show a decrease in SOC stocks under the disturbance scenario of high intensity thinning, compared to the control (Fig. 6). However, multi-model mean CO_2 fluxes also decrease in this scenario, compared to the control. This is probably due to lower C inputs and SOC stocks in this scenario (Fig. 5), which are directly linked to the respiration rates in the models (Eq. 2). In Fig. 7, we show the effect of different tree harvest intensities on the SOC stocks after 10 years, and relate those changes to the 10-year average C inputs. The harvest intensities were set as: control (MR = 0%), thinning (MR = 25%), high intensity thinning (MR = 50%), and clear-cutting (MR = 100%), always assuming a harvest rate of 100%. We can see that the reduction of SOC stocks due to tree harvest is proportional to the intensity of the treatment (Fig. 7). In particular, after 10 years, SOC is the lowest under the clear-cutting treatment ($MR_{100\%}$), followed by high intensity thinning ($MR_{50\%}$), thinning ($MR_{25\%}$) and control scenarios. Average C input changes follow a similar pattern, but reductions of C inputs are much sharper than the stocks (Fig. 7).

6.2. *Low effect of climate change*

For this 10-year simulation period, the effect of climate change in the control treatment is low, with SOC stocks being slightly higher under the RCP 6.0 scenario (Fig. 8). This difference is primarily driven by changes in predicted C inputs, which are higher on average under RCP 6.0 (Fig. B2). Changes in environmental conditions play a more limited direct effect: on average, slightly wetter conditions lead to a small increase in decomposition rates, while temperature changes induce a very small reduction in decomposition. The net effect of these opposing and relatively weak environmental responses is likely minor compared to the increase in C inputs, resulting in a small net accumulation of C in the soil. Overall, these results suggest that, over short time scales, modest shifts in climate lead to limited changes in decomposition dynamics, with SOC trends being mainly controlled by changes in C inputs.

6.3. *Large differences across models*

Despite a relatively modest decline in multi-model mean SOC stocks (i.e., a 2% decrease in SOC stocks after 10 years of simulation under the RCP 2.6 control scenario, relative to first year), we observed very large differences across models (Fig. 8). That is, SOC stock changes over the 10 years ranged between a 9% increase to a 22% decrease, with last year SOC stocks averaging 60.1 ± 7.6 Mg C ha^{-1} (multi-model mean ± standard deviation). These differences are consistent with previous studies highlighting model structural uncertainty (Farina et al., 2021; Bruni et al., 2022) and suggest that multi-model mean predictions should be interpreted carefully. Divergence among model outputs

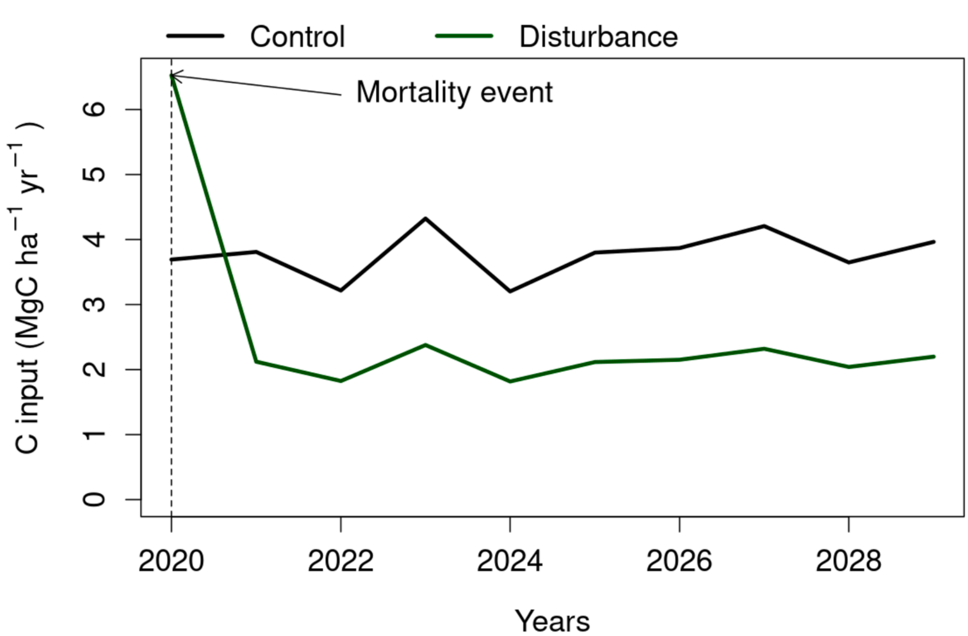

Fig. 5. (Downloaded from the web application) Evolution of carbon inputs over the 10-year simulation period for the control (black line) and land management (green line) scenarios.

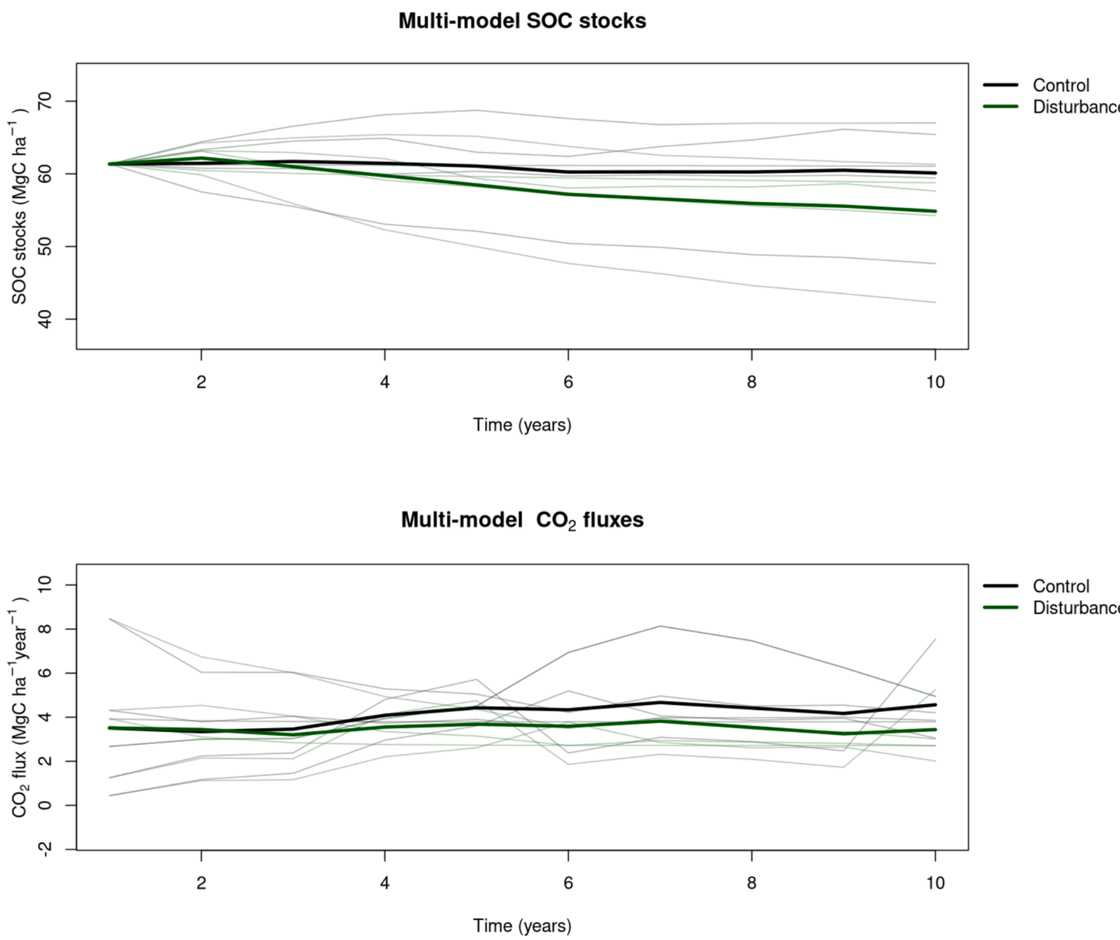

Fig. 6. (Downloaded from the web application) Ten-year evolution of SOC stocks and CO_2 fluxes in the French forestry site (45° 45′ 20’’ N, 2° 57′ 58" E) according to the control (black lines) and disturbance (green lines) scenarios. The bold lines represent the multi-model mean, while the shaded lines are the single model simulations.

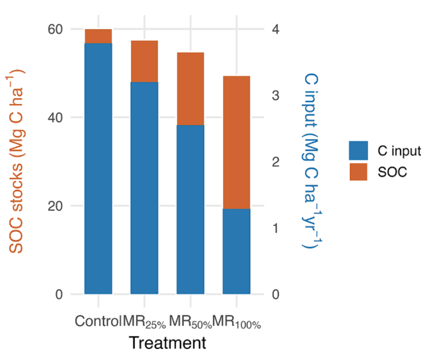

Fig. 7. SOC stocks after 10 years and 10-year average C inputs under different land management scenarios: control, 25% mortality rate ($MR_{25\%}$) 50% mortality rate ($MR_{50\%}$), and 100% mortality rate ($MR_{100\%}$), all assuming a 100% harvest rate of the plant residue.

derives from multiple sources, including differences in parametrization (Todd-Brown et al., 2013; Luo and Schuur, 2020; Bruni et al., 2024), model structure (Riggers et al., 2019; Bruni et al., 2022), and effects of the initialization (Yeluripati et al., 2009; Hashimoto et al., 2011). In our simulations, initial SOC stocks were estimated under the steady-state assumption and then rescaled to match observed values. This approach ensures realistic initial SOC levels but may bias initial model dynamics toward steady-state if the discrepancy between steady-state and observed SOC is large. Meanwhile, input data were standardized, minimizing the influence of forcing errors on model divergence. In the absence of thorough evaluation against observational data (Le Noë et al., 2023), the multi-model mean and its associated uncertainty offer the most comprehensive representation of SOC stock dynamics at the site level.

7. Further developments and limitations

7.1. Data input limitations

Data input from open-source databases is mainly intended to demonstrate the functionalities of the webtool rather than to provide robust site-specific simulations. The use of gridded datasets such as ISIMIP and LUCAS introduces uncertainty related to spatial resolution. Grid-cell averages may smooth local heterogeneity in climate, soil properties, and land-use, which can lead to discrepancies in SOC estimates. While a formal quantification of this effect is beyond the scope of the present study, previous work suggests that such aggregation can induce deviations in SOC estimates on the order of tens of percent (Wiltshire et al., 2024). In this context, the results obtained with open-source datasets should be interpreted as indicative rather than site-specific, and the use of local field measurements is expected to improve prediction accuracy.

While some datasets are reliable, such as climate projections from the ISIMIP models, others are more approximate and should be interpreted with caution. For example, vegetation data from ISIMIP simulations are extracted at the grid-cell level, which may include multiple

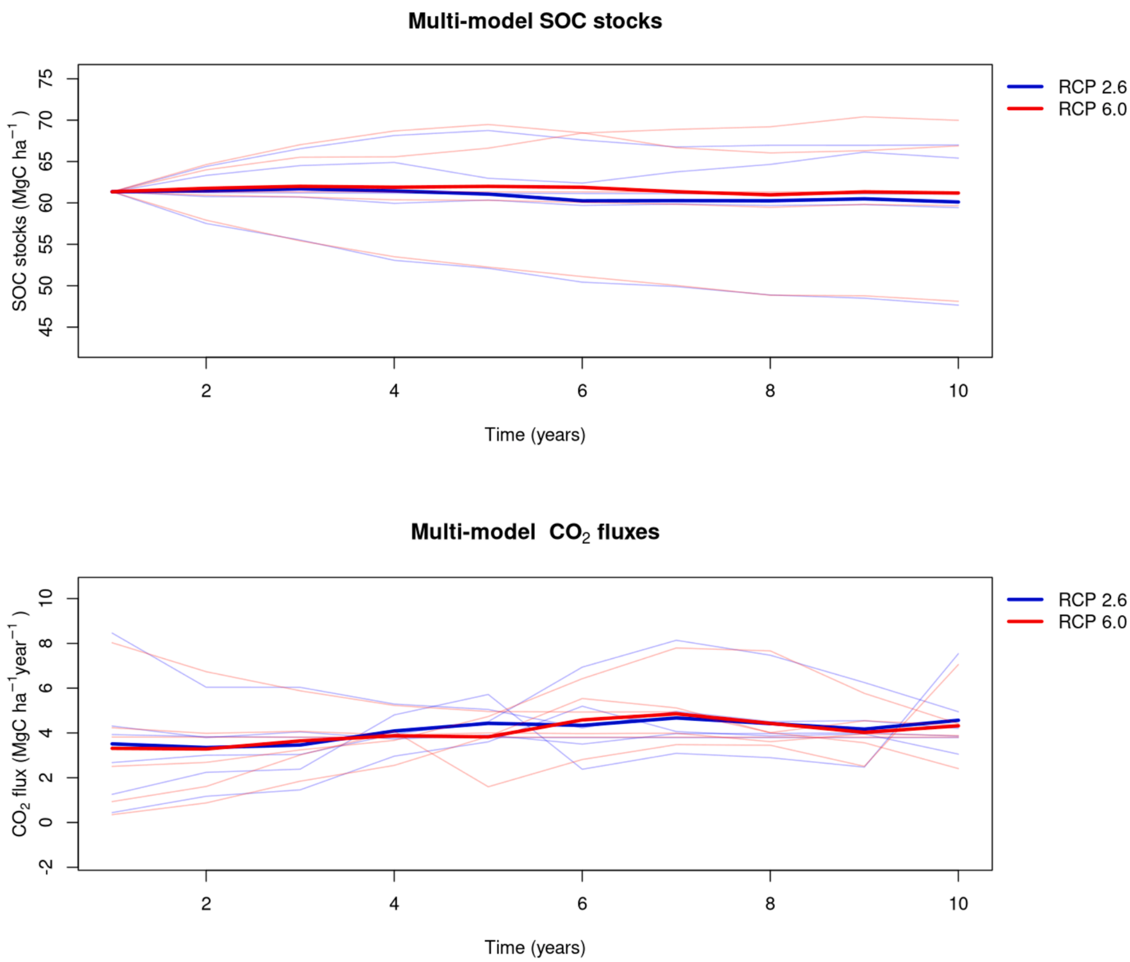

Fig. 8. (Downloaded from the web application) Ten-year evolution of SOC stocks and CO_2 fluxes in the French forestry site (45° 45′ 20′′ N, 2° 57′ 58" E) according to the RCP 2.6 (blue lines) and RCP 6.0 (red lines) climate change scenarios. The bold lines represent the multi-model mean, while the shaded lines are the single model simulations.

land-uses beyond forests. Moreover, ISIMIP vegetation models represent potential natural vegetation rather than managed ecosystems, such as those prevalent across Europe. This can lead to biases in estimates of actual C inputs to soils. This represents an important limitation that could be addressed in future versions of *me4soc*. In the current implementation, multi-model mean values of vegetation and climate variables are used to drive the SOC model ensemble. A more rigorous approach would be to run the SOC models separately for each vegetation and climate model to capture inter-model variability before averaging. However, this would require storing input data for each model and scenario, increasing the memory requirements for these datasets by approximately a factor of 112, and substantially increasing computational demands, thereby compromising the responsiveness of the app. Similar trade-off guided the selection of models from ISIMIP simulations. Considerations of computational efficiency also influenced the choice of SOC models. Although models incorporating explicit microbial processes and nonlinear kinetics are conceptually more mechanistic (e.g., Wieder et al., 2015; Abramoff et al., 2018), their need to solve nonlinear matrix equations makes them computationally demanding and less suited to interactive applications. For long-term projections, linear SOC models remain sufficiently robust, especially when combined via multi-model averages (Bruni et al., 2022). Overall, these design choices illustrate a common challenge in developing operational modeling tools: achieving an appropriate balance between incorporating process complexity, while maintaining computational efficiency and accessibility for end-users and practitioners.

7.2. *Initialization and parametrization*

The initialization protocol we used allows simulations to start from observed total SOC levels, which can substantially reduce initial model error (Hashimoto et al., 2011; Dimassi et al., 2018). However, the post–spin-up rescaling is likely to influence model trajectories, particularly in the short term. In practice, this adjustment can accelerate convergence toward model equilibrium behavior, potentially dampening transient dynamics.

Parametrization represents an additional source of uncertainty (Luo and Schuur, 2020). In *me4soc*, default parameter values were used, including transfer rates between compartments, parameters of the environmental response functions, and decomposition rate coefficients. Although these parameters are typically calibrated against observational datasets and assumed to be transferable, such datasets often span limited pedoclimatic conditions, and parameter values may not generalize across environments without adjustment.

While a full decomposition of uncertainty sources is beyond the scope of this study, multiple contributors to between-model variability can be identified, including initialization, parameterization, input data, and model structure (see e.g., Lehtonen and Heikkinen, 2016). With *me4soc*, structural uncertainty can be partially assessed by comparing simulations across models, whereas input data uncertainty can be explored by using alternative data sources (e.g., site-specific measurements versus large-scale open datasets).

7.3. Systematic validation of model outputs

There is a pressing need to improve methodologies for quantifying and reporting SOC changes in national GHG inventories (IPCC, 2006; Palosuo et al., 2025). However, robust predictions of SOC stocks and GHG fluxes require systematic validation of model performance against observational data (Le Noë et al., 2023). This often involves re-calibrating model parameters to match observed trends in SOC stocks and/or GHG emissions, and validation of model performance on independent data. While this calibration functionality is not yet implemented in the current version of *me4soc*, it is planned for future development of the web application. Users should note that successful calibration depends on the availability of multiple observations of SOC and/or GHG fluxes over time. As model complexity increases, the number of parameters to calibrate also rises—thereby requiring a proportional increase in the amount of observational data needed to ensure robust parameter estimation. The tool that we developed here is a simulation platform rather than a calibrated predictive system. Future developments should therefore prioritize systematic comparisons with observational data to strengthen robustness for predictive applications. For instance, in order to comply with the IPCC guidelines for national GHG inventories (IPCC, 2019), models should be tested and validated against local measurements (Bellassen et al., 2022), such as SOC stock changes and litterbag experiments, and associated uncertainties should be quantified.

Consistent with this approach, the European Carbon Removals and Carbon Farming (CRCF) regulation (European Union, 2024) adopts IPCC methodological principles as the basis for its certification framework. Implementing model performance estimates would also allow for more robust ensemble averaging than simple arithmetic means. For example, model outputs could be weighted based on their ability to predict available observations (Bruni et al., 2024; Sierra and Muñoz, 2025) or using Bayesian inference methods (Besic et al., 2025).

7.4. Generalization to global scale and other ecosystems

To make *me4soc* applicable at the global scale, the tool could be further developed to include open-source data available at the global scale, such as SoilGrids for soil parameters (Poggio et al., 2021). Other input data currently in *me4soc* are already available at the global scale (Table 1). However, expanding coverage to the entire global land area will require substantial increase in storage capacity for the additional data files.

Another avenue for development is the inclusion of ecosystems other than forests, such as croplands and grasslands. Except from SG, which was specifically designed for forest systems, the other models in the ensemble have been previously applied and evaluated in non-forested ecosystems (Garsia et al., 2023). Therefore, the extension of *me4soc* to croplands and grasslands would only require incorporating ecosystem-specific input data and land management practices (e.g., fertilizer application, use of cover crops, and crop species definition to set the litter input quality).

Future developments could also aim to implement more realistic and explicit management scenarios, as the current implementation is limited to simplified representations of tree mortality and litter retention (via mortality and harvest rates, respectively), allowing only a single perturbation per simulation. In addition, mixed-species systems can currently only be represented indirectly through adjustments of litter quality parameters, whereas a more explicit representation of species diversity effects could be incorporated in future developments.

8. Concluding remarks

Improving the robustness of SOC predictions and quantifying their uncertainties is paramount to better understand soil C feedbacks to climate change and to inform mitigation strategies through climate-smart land management practices. One of the main novelties of *me4soc* is to provide site-specific, scenario-based SOC projections using a multi-modeling approach, accessible via an intuitive and open-source web interface. This represents a first step toward offering an advanced SOC modeling platform to tackle decision-making needs, thereby supporting evidence-based forest management in the context of climate change. However, it is important to acknowledge the current limitations of the tool to correctly interpret its outputs. These include the use of default model parameters without re-calibration to local conditions, relying only on linear kinetic models, and the use of open-source input data (when not provided by the user), which have coarse resolution and may be inaccurate. The tool that we developed here is a simulation platform rather than a calibrated predictive system. Further developments include: 1) model evaluation through comparison with observational data to strengthen robustness for predictive applications, 2) extension of the applicability to the global scale and to other ecosystems; and 3) the integration of other models with more mechanistic representation of biogeochemical processes– while maintaining computational efficiency and usability for a broad range of stakeholders.

CRediT authorship contribution statement

Elisa Bruni: Writing – original draft, Visualization, Supervision, Software, Formal analysis, Conceptualization. **Aleksi Lehtonen:** Writing – review & editing, Funding acquisition, Conceptualization. **Shoji Hashimoto:** Writing – review & editing, Methodology. **Boris Ťupek:** Writing – review & editing, Methodology. **Nasser Bacha:** Software. **Daniel Bunker:** Data curation. **Illian Brasselet-Darracq:** Software. **Dalia Fages-Gouyou:** Software. **Yanis Hemeray:** Software. **Christopher P.O. Reyer:** Writing – review & editing. **Carlos A. Sierra:** Writing – review & editing. **Bertrand Guenet:** Writing – review & editing, Supervision, Funding acquisition, Conceptualization.

Declaration of competing interest

The authors declare that they have no known competing financial interests or personal relationships that could have appeared to influence the work reported in this paper.

Acknowledgements

This work has been supported by the grant Holistic management practices, modelling, and monitoring for European forest soils— HoliSoils (EU Horizon 2020 Grant Agreement No 101000289); by the Partnership for Research and Innovation in the Mediterranean Area ('the PRIMA Foundation') through the "Soil Health and Agriculture Resilience through an Integrated Geographical information systems of Mediterranean Drylands" project (Grant Agreement No 2211) (SHARInG-MeD); and by the project ALAMOD of the exploratory research program FairCarboN and received French government funding managed by the Agence Nationale de la Recherche under the France 2030 program, reference ANR-22-PEXF-0002. We acknowledge the TRY Initiative on Plant Traits and especially the contribution of Isabelle Aubin for the TRY data used in this publication.

Appendix A

Table A1
List of input variables, including their units, definitions, and the open-source databases used to extract or estimate them when user-provided data are unavailable (for Europe only).

Variable	Type	Unit	Definition	Open-source database	Extracted/ estimated
GPS latitude	Simulation setup	Decimal degrees	GPS latitude of the study site		
GPS longitude	Simulation setup	Decimal degrees	GPS longitude of the study site		
Simulation length	Simulation setup	Number of years	Duration of the simulation period		
Initial simulation date	Simulation setup	Date (YY-MM-DD)	Starting date of the simulations		
Clay	Soil	%	Soil clay concentration	LUCAS	Extracted
Silt	Soil	%	Soil silt concentration	LUCAS	Extracted
Initial SOC stock	Soil	Mg C ha^{-1}	Soil organic carbon stock at the beginning of the simulation period	LUCAS	Extracted
Soil layer thickness	Soil	cm	Thickness of the organic layer		
C:N ratio	Soil	g C g N^{-1}		LUCAS	Extracted
Bulk density	Soil	Mg m^{-3}	Soil bulk density	LUCAS	Extracted
Dominant species	Litter input		Dominant tree species		
Annual aboveground C input	Litter input	Mg C ha^{-1} yr^{-1}	Time series of the level of aboveground C input to the soil	ISIMIP, multi-model average	Estimated
Annual belowground C input	Litter input	Mg C ha^{-1} yr^{-1}	Time series of the level of belowground C input to the soil	ISIMIP, multi-model average	Estimated
Acid hydrolysable compounds fraction	Litter input	g g^{-1}	Acid hydrolysable compounds of the litter input	Yasso07 manual	Extracted
Water soluble compounds fraction	Litter input	g g^{-1}	Water soluble compounds of the litter input	Yasso07 manual	Extracted
Ethanol soluble compounds fraction	Litter input	g g^{-1}	Ethanol soluble compounds of the litter input	Yasso07 manual	Extracted
Neither soluble nor hydrolysable compounds fraction	Litter input	g g^{-1}	Neither soluble nor hydrolysable compounds of the litter input	Yasso07 manual	Extracted
Lignin:nitrogen ratio	Litter input	g g N^{-1}	Lignin to nitrogen ratio of the litter input	C:N from TRY, %C from Ma et al., 2018, lignin from Yasso07 manual	Estimated
Lignin fraction	Litter input	g g^{-1}	Lignin fraction in the litter input	Considered equivalent to the neither soluble nor hydrolysable compounds fraction from the Yasso07 manual	Extracted
Woody litter size	Litter input	cm	Diameter of the woody litter	Tuomi et al., 2009	Extracted
Daily surface temperature	Climate	°C	Daily surface temperature during the simulation length	ISIMIP, multi-model average	Extracted
Spin-up surface temperature	Climate	°C	Daily average surface temperature in the decades preceding the simulation	ISIMIP, multi-model average	Extracted
Daily precipitation	Climate	mm	Daily precipitation during the simulation length	ISIMIP, multi-model average	Extracted
Spin-up precipitation	Climate	mm	Daily average precipitation in the decades preceding the simulation	ISIMIP, multi-model average	Extracted
Monthly potential evapotranspiration	Climate	mm	Monthly potential evapotranspiration during the simulation length	ISIMIP, multi-model average	Extracted
Spin-up potential evapotranspiration	Climate	mm	Monthly average potential evapotranspiration in the decades preceding the simulation	ISIMIP, multi-model average	Extracted
Daily volumetric soil water content	Climate	mm^3 mm^{-3}	Daily volumetric soil water content during the simulation length	ISIMIP, multi-model average	Extracted
Spin-up volumetric soil water content	Climate	mm^3 mm^{-3}	Daily average volumetric soil water content in the decades preceding the simulation	ISIMIP, multi-model average	Extracted
Atmospheric CH_4 concentration	Climate	ppb	Atmospheric CH_4 concentration at the beginning of the simulations	GML	Extracted
Year of disturbance event	Land management		Number of the year of the disturbance event		
Aboveground biomass	Land management	Mg C ha^{-1} yr^{-1}	Amount of the plant aboveground biomass in the year preceding the disturbance event	ISIMIP, multi-model average	Estimated
Belowground biomass	Land management	Mg C ha^{-1} yr^{-1}	Amount of the plant belowground biomass in the year preceding the disturbance event	ISIMIP, multi-model average	Estimated
Mortality rate	Land management	%	Percentage of vegetation died during the disturbance event		
Harvest rate	Land management	%	Harvest rate of the dead aboveground biomass		

Appendix B

Fig. B1

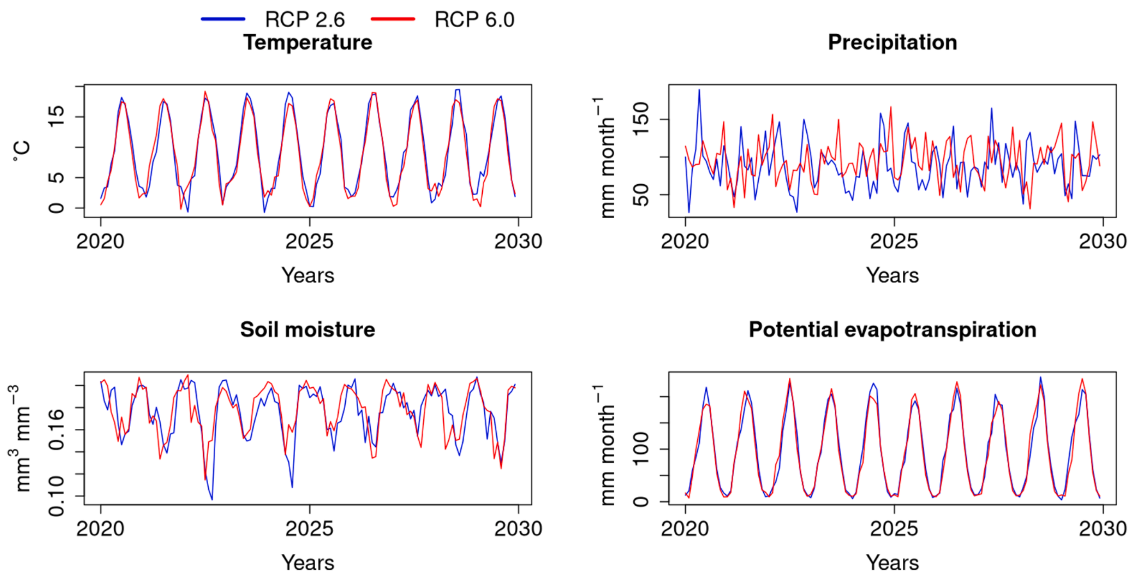

Fig. B1. shows ISIMIP multi-model mean air temperature, precipitation, soil moisture and potential evapotranspiration, under climate change scenarios RCP 2.6 and RCP 6.0. This data is used as input to the SOC models for the 10-year simulations at the French forestry site (45° 45′ 20'' N, 2° 57′ 58" E).

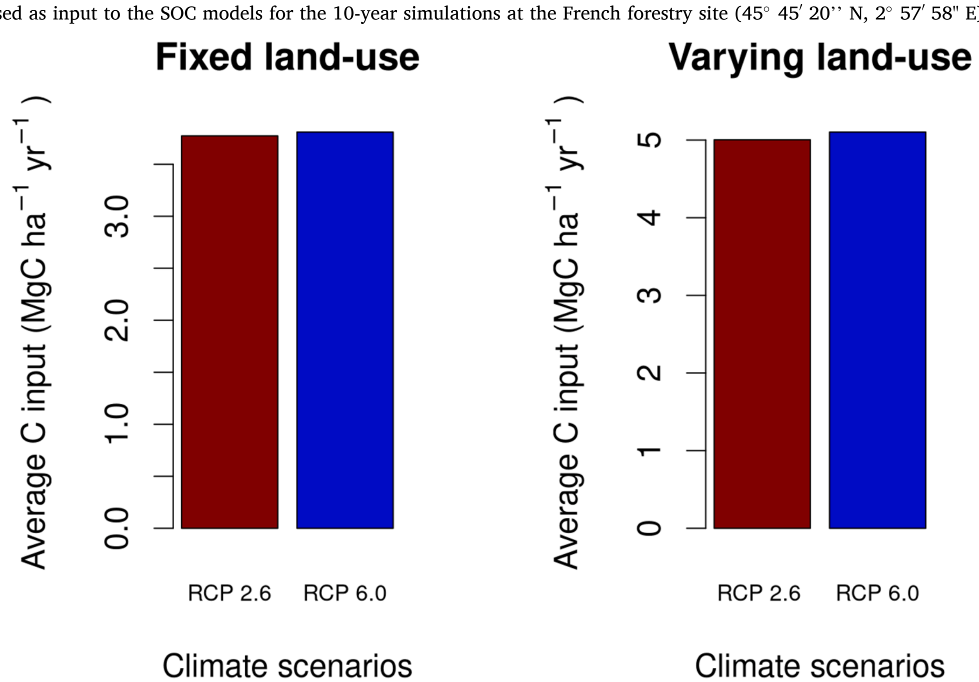

Fig. B2. (Downloaded from the web application) 10-year average C inputs at the French forestry site (45° 45′ 20'' N, 2° 57′ 58" E), extracted from ISIMIP multi-model mean simulations under climate change scenarios RCP 2.6 and RCP 6.0, and under fixed and varying land-use scenarios.

Data availability

https://github.com/elisabruni/me4soc (All webapp code and test-site data is available at:)

Reference

Abramoff, R., Xu, X., Hartman, M., O'Brien, S., Feng, W., Davidson, E., Finzi, A., Moorhead, D., Schimel, J., Torn, M., Mayes, M.A., 2018. The Millennial model: in search of measurable pools and transformations for modeling soil carbon in the new century. Biogeochemistry 137, 51–71. https://doi.org/10.1007/s10533-017-0409-7.

Andrén, O., Kätterer, T., 1997. Icbm: The introductory carbon balance model for exploration of soil carbon balances. Ecol. Appl. 7, 1226–1236. https://doi.org/10.1890/1051-0761(1997)007%5B1226:ITICBM%5D2.0.CO;2.

Ballabio, C., Lugato, E., Fernández-Ugalde, O., Orgiazzi, A., Jones, A., Borrelli, P., Montanarella, L., Panagos, P., 2019. Mapping LUCAS topsoil chemical properties at European scale using gaussian process regression. Geoderma 355, 113912. https://doi.org/10.1016/j.geoderma.2019.113912.

Ballabio, C., Panagos, P., Monatanarella, L., 2016. Mapping topsoil physical properties at European scale using the LUCAS database. Geoderma 261, 110–123. https://doi.org/10.1016/j.geoderma.2015.07.006.

Bellassen, V., Angers, D., Kowalczewski, T., Olesen, A., 2022. Soil carbon is the blind spot of European national GHG inventories. Nat. Clim. Chang 12, 324–331. https://doi.org/10.1038/s41558-022-01321-9.

Besic, N., Picard, N., Vega, C., Bontemps, J.-D., Hertzog, L., Renaud, J.-P., Fogel, F., Schwartz, M., Pellissier-Tanon, A., Destouet, G., Mortier, F., Planells-Rodriguez, M., Ciais, P., 2025. Remote-sensing-based forest canopy height mapping: some models

are useful, but might they provide us with even more insights when combined? Geosci. Model Dev. 18, 337–359. https://doi.org/10.5194/gmd-18-337-2025.
Bruni, E., Chenu, C., Abramoff, R.Z., Baldoni, G., Barkusky, D., Clivot, H., Huang, Y., Kätterer, T., Pikuła, D., Spiegel, H., Virto, I., Guenet, B., 2022. Multi-modelling predictions show high uncertainty of required carbon input changes to reach a 4‰ target. Eur. J. Soil Sci. 73. https://doi.org/10.1111/ejss.13330.
Bruni, E., Lugato, E., Chenu, C., Guenet, B., 2024. European croplands under climate change: carbon input changes required to increase projected soil organic carbon stocks. Sci. Total Environ. 954, 176525. https://doi.org/10.1016/j.scitotenv.2024.176525.
Coleman, K., Jenkinson, D.S., 1996. RothC-26.3 - A model for the turnover of carbon in soil. In: Powlson, D.S., Smith, P., Smith, J.U. (Eds.), Evaluation of Soil Organic Matter Models. Springer Berlin Heidelberg, Berlin, Heidelberg, pp. 237–246. https://doi.org/10.1007/978-3-642-61094-3_17.
De Brogniez, D., Ballabio, C., Stevens, A., Jones, R.J.A., Montanarella, L., Van Wesemael, B., 2015. A map of the topsoil organic carbon content of Europe generated by a generalized additive model. Eur. J. Soil Sci. 66, 121–134. https://doi.org/10.1111/ejss.12193.
Dimassi, B., Guenet, B., Saby, N.P.A., Munoz, F., Bardy, M., Millet, F., Martin, M.P., 2018. The impacts of CENTURY model initialization scenarios on soil organic carbon dynamics simulation in French long-term experiments. Geoderma 311, 25–36. https://doi.org/10.1016/j.geoderma.2017.09.038.
European Union, 2024. Regulation (EU) 2024/3012 of the European Parliament and of the Council of 27 November 2024 establishing a Union certification framework for permanent carbon removals, carbon farming and carbon storage in products. Off. J. Eur. Union L, 6.12.2024. https://eur-lex.europa.eu/eli/reg/2024/3012/oj/eng.
Farina, R., Sándor, R., Abdalla, M., Álvaro-Fuentes, J., Bechini, L., Bolinder, M.A., Brilli, L., Chenu, C., Clivot, H., De Antoni Migliorati, M., Bene, C.D., Dorich, C.D., Ehrhardt, F., Ferchaud, F., Fitton, N., Francaviglia, R., Franko, U., Giltrap, D.L., Grant, B.B., Guenet, B., Harrison, M.T., Kirschbaum, M.U.F., Kuka, K., Kulmala, L., Liski, J., McGrath, M.J., Meier, E., Menichetti, L., Moyano, F., Nendel, C., Recous, S., Reibold, N., Shepherd, A., Smith, W.N., Smith, P., Soussana, J.-F., Stella, T., Taghizadeh-Toosi, A., Tsutskikh, E., Bellocchi, G., 2021. Ensemble modelling, uncertainty and robust predictions of organic carbon in long-term bare-fallow soils. Glob. Change Biol. 27, 904–928. https://doi.org/10.1111/gcb.15441.
Friedlingstein, P., O'Sullivan, M., Jones, M.W., Andrew, R.M., Hauck, J., Landschützer, P., Le Quéré, C., Li, H., Luijkx, I.T., Olsen, A., Peters, G.P., Peters, W., Pongratz, J., Schwingshackl, C., Sitch, S., Canadell, J.G., Ciais, P., Jackson, R.B., Alin, S.R., Arneth, A., Arora, V., Bates, N.R., Becker, M., Bellouin, N., Berghoff, C.F., Bittig, H.C., Bopp, L., Cadule, P., Campbell, K., Chamberlain, M.A., Chandra, N., Chevallier, F., Chini, L.P., Colligan, T., Decayeux, J., Djeutchouang, L.M., Dou, X., Duran Rojas, C., Enyo, K., Evans, W., Fay, A.R., Feely, R.A., Ford, D.J., Foster, A., Gasser, T., Gehlen, M., Gkritzalis, T., Grassi, G., Gregor, L., Gruber, N., Gürses, Ö., Harris, I., Hefner, M., Heinke, J., Hurtt, G.C., Iida, Y., Ilyina, T., Jacobson, A.R., Jain, A.K., Jarníková, T., Jersild, A., Jiang, F., Jin, Z., Kato, E., Keeling, R.F., Klein Goldewijk, K., Knauer, J., Korsbakken, J.I., Lan, X., Lauvset, S.K., Lefèvre, N., Liu, Z., Liu, J., Ma, L., Maksyutov, S., Marland, G., Mayot, N., McGuire, P.C., Metzl, N., Monacci, N.M., Morgan, E.J., Nakaoka, S.-I., Neill, C., Niwa, Y., Nützel, T., Olivier, L., Ono, T., Palmer, P.I., Pierrot, D., Qin, Z., Resplandy, L., Roobaert, A., Rosan, T.M., Rödenbeck, C., Schwinger, J., Smallman, T.L., Smith, S.M., Sospedra-Alfonso, R., Steinhoff, T., Sun, Q., Sutton, A.J., Séférian, R., Takao, S., Tatebe, H., Tian, H., Tilbrook, B., Torres, O., Tourigny, E., Tsujino, H., Tubiello, F., Van Der Werf, G., Wanninkhof, R., Wang, X., Yang, D., Yang, X., Yu, Z., Yuan, W., Yue, X., Zaehle, S., Zeng, N., Zeng, J., 2025. Global Carbon Budget 2024. Earth Syst. Sci. Data 17, 965–1039. https://doi.org/10.5194/essd-17-965-2025.
Frieler, K., Lange, S., Piontek, F., Reyer, C.P.O., Schewe, J., Warszawski, L., Zhao, F., Chini, L., Denvil, S., Emanuel, K., Geiger, T., Halladay, K., Hurtt, G., Mengel, M., Murakami, D., Ostberg, S., Popp, A., Riva, R., Stevanovic, M., Suzuki, T., Volkholz, J., Burke, E., Ciais, P., Ebi, K., Eddy, T.D., Elliott, J., Galbraith, E., Gosling, S.N., Hattermann, F., Hickler, T., Hinkel, J., Hof, C., Huber, V., Jägermeyr, J., Krysanova, V., Marcé, R., Müller Schmied, H., Mouratiadou, I., Pierson, D., Tittensor, D.P., Vautard, R., van Vliet, M., Biber, M.F., Betts, R.A., Bodirsky, B.L., Deryng, D., Frolking, S., Jones, C.D., Lotze, H.K., Lotze-Campen, H., Sahajpal, R., Thonicke, K., Tian, H., Yamagata, Y., 2017. Assessing the impacts of 1.5°C global warming – simulation protocol of the Inter-Sectoral Impact Model Intercomparison Project (ISIMIP2b). Geosci. Model Dev. 10, 4321–4345. https://doi.org/10.5194/gmd-10-4321-2017.
Garsia, A., Moinet, A., Vazquez, C., Creamer, R.E., Moinet, G.Y.K., 2023. The challenge of selecting an appropriate soil organic carbon simulation model: A comprehensive global review and validation assessment. Glob. Change Biol. gcb, 16896. https://doi.org/10.1111/gcb.16896.
Hashimoto, S., 2012. A new estimation of global soil greenhouse gas fluxes using a simple data-oriented model. PLoS ONE 7, e41962. https://doi.org/10.1371/journal.pone.0041962.
Hashimoto, Shoji, Morishita, T., Sakata, T., Ishizuka, S., Kaneko, S., Takahashi, M., 2011. Simple models for soil CO2, CH4, and N2O fluxes calibrated using a bayesian approach and multi-site data. Ecol. Model. 11.
Hashimoto, S., Wattenbach, M., Smith, P., 2011. A new scheme for initializing process-based ecosystem models by scaling soil carbon pools. Ecol. Model. 222, 3598–3602. https://doi.org/10.1016/j.ecolmodel.2011.08.011.
Hidy, D., Barcza, Z., Marjanović, H., Ostrogović Sever, M.Z., Dobor, L., Gelybó, G., Fodor, N., Pintér, K., Churkina, G., Running, S., Thornton, P., Bellocchi, G., Haszpra, L., Horváth, F., Suyker, A., Nagy, Z., 2016. Terrestrial ecosystem process model biome-BGCMuSo v4.0: summary of improvements and new modeling possibilities. Geosci. Model Dev. 9, 4405–4437. https://doi.org/10.5194/gmd-9-4405-2016.
IPCC, 2006. 2006 IPCC Guidelines for National Greenhouse Gas Inventories, Prepared by the National Greenhouse Gas Inventories Programm. Institute for Global Environmental Strategies, Hayama.
IPCC, 2019. . Chapter 2 generic methodologies applicable to multiple land-use categories. In: Ogle, S.M., et al. (Eds.), Refinement to the 2006 IPCC Guidelines for National Greenhouse Gas Inventories, pp. 2.1–2.96, 2019.
Jackson, R.B., Lajtha, K., Crow, S.E., Hugelius, G., Kramer, M.G., Piñeiro, G., 2017. The ecology of soil carbon: pools, vulnerabilities, and biotic and abiotic controls. Annu. Rev. Ecol. Evol. Syst. 48, 419–445. https://doi.org/10.1146/annurev-ecolsys-112414-054234.
Jonard, M., Nicolas, M., Coomes, D.A., Caignet, I., Saenger, A., Ponette, Q., 2017. Forest soils in France are sequestering substantial amounts of carbon. Sci. Total Environ. 574, 616–628. https://doi.org/10.1016/j.scitotenv.2016.09.028.
Kattge, J., Bönisch, G., Díaz, S., Lavorel, S., Prentice, I.C., Leadley, P., Tautenhahn, S., Werner, G., 2020. TRY plant trait database – enhanced coverage and open access. Glob. Change Biol. 26, 119–188. https://doi.org/10.1111/gcb.14904.
Konôpka, B., Jozef, P., Vladimír, Š., Peter, S., Katarína, M., 2021. Woody and foliage biomass, foliage traits and growth efficiency in young trees of four broadleaved tree species in a temperate forest. Plants 10 (10), 2155. https://doi.org/10.3390/plants10102155.
Krinner, G., Viovy, N., de Noblet-Ducoudré, N., Ogée, J., Polcher, J., Friedlingstein, P., Ciais, P., Sitch, S., Prentice, I.C., 2005. A dynamic global vegetation model for studies of the coupled atmosphere-biosphere system: DVGM FOR COUPLED CLIMATE STUDIES. Glob. Biogeochem. Cycles 19. https://doi.org/10.1029/2003GB002199.
Lal, R., 2008. Carbon sequestration. Philos. Trans. R. Soc. B: Biol. Sci. 363, 815–830. https://doi.org/10.1098/rstb.2007.2185.
Lal, R., 2004. Soil carbon sequestration impacts on global climate change and food security. Final Front. 304.
Lan, X., Thoning, K.W., Dlugokencky, E.J., 2022. Trends in globally-averaged CH4, N2O, and SF6 determined from NOAA Global Monitoring Laboratory measurements.
Lehtonen, A., Heikkinen, J., 2016. Uncertainty of upland soil carbon sink estimate for Finland. Can. J. For, Res 46 (3), 310–322. https://doi.org/10.1139/cjfr-2015-0171.
Le Noë, J., Manzoni, S., Abramoff, R., Bölscher, T., Bruni, E., Cardinael, R., Ciais, P., Chenu, C., Clivot, H., Derrien, D., 2023. Soil organic carbon models need independent time-series validation for reliable prediction. Commun. Earth Environ. 4, 158.
Liski, J., Tuomi, M., Rasinmäki, J., 2009. Yasso07 user-interface manual.
Luo, Y., Schuur, E.A.G., 2020. Model parameterization to represent processes at unresolved scales and changing properties of evolving systems. Glob. Change Biol. 26, 1109–1117. https://doi.org/10.1111/gcb.14939.
Mäkipää, R., 2023. How Does Management Affect Soil C Sequestration and Greenhouse Gas Fluxes in Boreal and Temperate Forests? – A Review. Forest Ecology and Management.
Malhi, Y., Doughty, C., Galbraith, D., 2011. The allocation of ecosystem net primary productivity in tropical forests. Philos. Trans. R. Soc. B: Biol. Sci. 366, 3225–3245. https://doi.org/10.1098/rstb.2011.0062.
Manzoni, S., Piñeiro, G., Jackson, R.B., Jobbágy, E.G., Kim, J.H., Porporato, A., 2012. Analytical models of soil and litter decomposition: solutions for mass loss and time-dependent decay rates. Soil Biol. Biochem. 50, 66–76. https://doi.org/10.1016/j.soilbio.2012.02.029.
Masson-Delmotte, V., Zhai, P., Pirani, A., Connors, S.L., Péan, C., Berger, S., Caud, N., Chen, Y., Goldfarb, L., Gomis, M.I., Huang, M., Leitzell, K., Lonnoy, E., Matthews, J. B.R., Maycock, T.K., Waterfield, T., Yelekçi, O., Yu, R., Zhou, B., 2021. Climate Change 2021: the physical science basis. In: Contribution of Working Group I to the Sixth Assessment Report of the Intergovernmental Panel on Climate Change.
Neumann, M., Ukonmaanaho, L., Johnson, J., Benham, S., Vesterdal, L., Novotný, R., Verstraeten, A., Lundin, L., Thimonier, A., Michopoulos, P., Hasenauer, H., 2018. Quantifying carbon and nutrient input from litterfall in European forests using field observations and modeling. Glob. Biogeochem. Cycles 32, 784–798. https://doi.org/10.1029/2017GB005825.
Intergovernmental Panel on Climate Change, 2015. In: Pachauri, R.K., Mayer, L. (Eds.), Climate Change 2014: Synthesis Report. Intergovernmental Panel on Climate Change, Geneva, Switzerland.
Palosuo, T., Heikkinen, J., Hilasvuori, E., Kulmala, L., Launiainen, S., Lehtilä, A., Leinonen, I., Liimatainen, M., Salminen, M., Shurpali, N., Silfver, T., Soinne, H., Vira, J., Liski, J., 2025. Demands and possibilities for field-scale estimation of agricultural greenhouse gas balances. CATENA 249, 108649. https://doi.org/10.1016/j.catena.2024.108649.
Pan, Y., Birdsey, R.A., Phillips, O.L., Houghton, R.A., Fang, J., Kauppi, P.E., Keith, H., Kurz, W.A., Ito, A., Lewis, S.L., Nabuurs, G.-J., Shvidenko, A., Hashimoto, S., Lerink, B., Schepaschenko, D., Castanho, A., Murdiyarso, D., 2024. The enduring world forest carbon sink. Nature 631, 563–569. https://doi.org/10.1038/s41586-024-07602-x.
Parton, W.J., Stewart, J.W.B., Cole, C.V., 1988. Dynamics of C, N, P and S in grassland soils: a model. Biogeochemistry 5, 109–131. https://doi.org/10.1007/BF02180320.
Poggio, L., De Sousa, L.M., Batjes, N.H., Heuvelink, G.B.M., Kempen, B., Ribeiro, E., Rossiter, D., 2021. SoilGrids 2.0: producing soil information for the globe with quantified spatial uncertainty. SOIL 7, 217–240. https://doi.org/10.5194/soil-7-217-2021.
R Core Team, 2022. R: A language and environment for statistical computing.
Reyer, C., Chang, J., Chen, M., Forrest, M., François, L., Henrot, A.-J., Hickler, T., Ito, A., Nishina, K., Ostberg, S., Schaphoff, S., Seneviratne, S.I., Shi, H., Steinkamp, J., Thiery, W., Tian, H., Zhao, F., Büchner, M., Ciais, P., 2019. ISIMIP2b Simulation data from biomes sector. 10.5880/PIK.2019.012.

Riggers, C., Poeplau, C., Don, A., Bamminger, C., Höper, H., Dechow, R., 2019. Multi-model ensemble improved the prediction of trends in soil organic carbon stocks in German croplands. Geoderma 345, 17–30. https://doi.org/10.1016/j.geoderma.2019.03.014.

Sierra, C.A., Müller, M., Trumbore, S.E., 2012. Models of soil organic matter decomposition: the SoilR package, version 1.0. Geosci. Model Dev. 5, 1045–1060. https://doi.org/10.5194/gmd-5-1045-2012.

Sierra, C.A., Muñoz, E., 2025. An information-theoretic approach to obtain ensemble averages from Earth system models. Geosci. Model Dev. 18, 6701–6716. https://doi.org/10.5194/gmd-18-6701-2025.

Smith, P., Soussana, J., Angers, D., Schipper, L., Chenu, C., Rasse, D.P., Batjes, N.H., Van Egmond, F., McNeill, S., Kuhnert, M., Arias-Navarro, C., Olesen, J.E., Chirinda, N., Fornara, D., Wollenberg, E., Álvaro-Fuentes, J., Sanz-Cobena, A., Klumpp, K., 2020. How to measure, report and verify soil carbon change to realize the potential of soil carbon sequestration for atmospheric greenhouse gas removal. Glob. Change Biol. 26, 219–241. https://doi.org/10.1111/gcb.14815.

Todd-Brown, K.E.O., Randerson, J.T., Post, W.M., Hoffman, F.M., Tarnocai, C., Schuur, E. A.G., Allison, S.D., 2013. Causes of variation in soil carbon simulations from CMIP5 Earth system models and comparison with observations. Biogeosciences 10, 1717–1736. https://doi.org/10.5194/bg-10-1717-2013.

Tuomi, M., Thum, T., Järvinen, H., Fronzek, S., Berg, B., Harmon, M., Trofymow, J.A., Sevanto, S., Liski, J., 2009. Leaf litter decomposition—Estimates of global variability based on Yasso07 model. Ecol. Model. 220, 3362–3371. https://doi.org/10.1016/j.ecolmodel.2009.05.016.

Varney, R.M., Chadburn, S.E., Burke, E.J., Cox, P.M., 2022. Evaluation of soil carbon simulation in CMIP6 earth system models. Biogeosciences 19, 4671–4704. https://doi.org/10.5194/bg-19-4671-2022.

Viskari, T., Pusa, J., Fer, I., Repo, A., Vira, J., Liski, J., 2022. Calibrating the soil organic carbon model Yasso20 with multiple datasets. Geosci. Model Dev. 15, 1735–1752. https://doi.org/10.5194/gmd-15-1735-2022.

Wieder, W.R., Allison, S.D., Davidson, E.A., Georgiou, K., Hararuk, O., He, Y., Hopkins, F., Luo, Y., Smith, M.J., Sulman, B., Todd-Brown, K., Wang, Y.-P., Xia, J., Xu, X., 2015. Explicitly representing soil microbial processes in earth system models: soil microbes in earth system models. Glob. Biogeochem. Cycles 29, 1782–1800. https://doi.org/10.1002/2015GB005188.

Wiltshire, S., Clemins, P.J., Beckage, B., 2024. Granularity of model input data impacts estimates of carbon storage in soils. PLoS Clim. 3, e0000363. https://doi.org/10.1371/journal.pclm.0000363.

Yeluripati, J.B., Van Oijen, M., Wattenbach, M., Neftel, A., Ammann, A., Parton, W.J., Smith, P., 2009. Bayesian calibration as a tool for initialising the carbon pools of dynamic soil models. Soil Biol. Biochem. 41, 2579–2583. https://doi.org/10.1016/j.soilbio.2009.08.021.

Yigini, Y., Panagos, P., 2016. Assessment of soil organic carbon stocks under future climate and land cover changes in Europe. Sci. Total Environ. 557–558, 838–850. https://doi.org/10.1016/j.scitotenv.2016.03.085.